ELSEVIER

Sensors and Actuators A 101 (2002) 364–370

SENSORS AND ACTUATORS A PHYSICAL

www.elsevier.com/locate/sna

The influences of the material properties on ceramic micro-stereolithography

Cheng Sun, Xiang Zhang*

Department of Mechanical and Aerospace Engineering, University of California at Los Angeles, 48-121 Engineering IV, Los Angeles, CA 90095, USA

Received 11 April 2002; received in revised form 28 June 2002; accepted 3 July 2002

Abstract

Ceramic micro-stereolithography (μSL) was recently introduced in the fabrication of complex 3D ceramic microstructures. Light scattering is found as an important factor in the μSL of ceramics. In this work, the Monte Carlo ray tracing method is employed to investigate the influences of the important materials properties on the scattering during the ceramic μSL. It is found that the scattering is the strongest when the size of the ceramic powders approaches to the laser wavelength (0.364 μm). It was also found that the higher the refractive index contrast between the particle and the resin, the stronger the light scattering. High laser intensity is required to fabricate absorbing ceramic materials to compensate for the laser energy absorbed by the ceramic particle. The μSL of three typical ceramic powders: silica, alumina, and lead zirconate titanate (PZT) are examined by the numerical model. The numerical model has been demonstrated as an efficient tool to optimize the μSL process. Finally, the ceramic micro green structures have been successfully fabricated.
© 2002 Elsevier Science B.V. All rights reserved.

Keywords: Micro-stereolithography; Monte Carlo simulation; Microfabrication; Ceramic; Polymer

1. Introduction

Ceramics are known for its excellent temperature and chemical resistance, high value of hardness, low thermal conductivity, ferroelectricity, etc. Many investigations have been conducted on the application of ceramics as a functional and/or structural material in micro-electromechanics systems (MEMS) [1–4]. Various novel ceramic microfabrication approaches, such as micro-extrusion [5], screen printing [6], jet molding [7], and LIGA based injection molding [8], have been developed. However, these processes are mainly used to fabricate 2D or 2.5D structures, which may greatly limit the performance of ceramic MEMS devices. Micro-stereolithography (μSL) was recently introduced to fabricate the complex 3D ceramic parts [9,10].

μSL is a microfabrication process based on the spatially resolved laser polymerization in the UV-curable solution [9]. 3D microstructures are fabricated in a layer-by-layer fashion according to designed CAD solid models [11]. In the ceramic μSL, ceramic green structures are fabricated from a UV-curable solution containing monomer, photoinitiator, ceramic particle, dispersant and UV absorber [10,12,13]. The dense ceramic micro parts can be obtained from green structures following the binder removal and sintering processes. In order to avoid deformation and cracking during binder removal, reduce the shrinkage during the sintering, and fabricate the homogenized and dense ceramics part, a solid loading of larger than 50% (volume ratio) is necessary [14].

Fig. 1 depicts the principle of a recently developed ceramics μSL apparatus [9]. Using this system, fabrication of fine 3D complex alumina and lead zirconate titanate (PZT) microstructures have been demonstrated [10]. Experiments indicated that curing depth and curing radius are the two critical parameters in μSL. In general, smaller curing depth and curing radius are desired to achieve high spatial resolution. However, a minimal curing depth and curing radius are required to ensure strong bonding within the whole microstructure [10]. It was found that light scattering due to the particles suspended in monomer solution is the most important mechanism determining the spatial resolutions of μSL (Fig. 2). In-depth understanding of the fundamental physics of scattering and photochemistry involved in the ceramic μSL is important to the process. A numerical model based on Monte Carlo simulation has been developed to investigate the light propagation, scattering and photopolymerization in highly concentrated ceramic suspensions.

* Corresponding author. Tel.: +1-310-206-7699; fax: +1-310-206-2302.
E-mail address: xiang@seas.ucla.edu (X. Zhang).

0924-4247/02/$ – see front matter © 2002 Elsevier Science B.V. All rights reserved.
PII: S0924-4247(02)00264-9

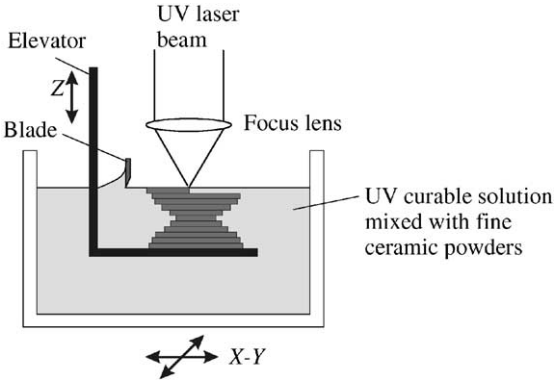

Fig. 1. Schematic diagram of ceramic μSL apparatus. In additional to the standard μSL setup, a precision blade has been implemented to define a flat thin layer of the viscous ceramic resin.

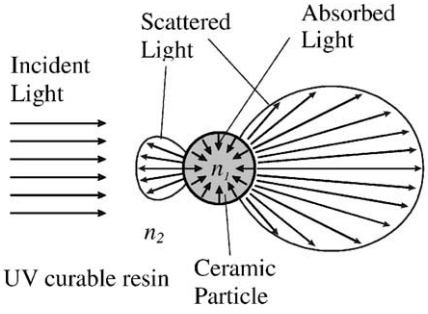

Fig. 2. Schematic diagram shows how light scattering and absorption occurs within the optically inhomogeneous media, which contains ceramic particles with refractive index of n_1 and the UV-curable resin with the refractive index of n_2.

This model has been successfully applied to investigate the doping effects as well in ceramic μSL [15]. However, as suggested by experiments, other physical parameters also strongly affect the ceramic μSL process [10,12,13].

In this work, a numerical model is used to study the spatial resolution of μSL process by evaluating the influences of various physical parameters, such as refractive indices of UV-curable solution and ceramic particles, ceramic particle size and distribution, and the absorbing nature of the ceramic particles. μSL of three typical ceramic materials: silica, alumina, and PZT, are investigated numerically (Table 1).

Table 1
Numerical parameters

Gaussian radius of laser beam	$w_0 = 4 \times 10^{-6}$ m
Monomer initial concentration	4.46×10^3 mol/m^3
Density of HDDA	$\rho = 1.01$ kg/m^3
Photoinitiator initial concentration	2.23×10^2 mol/m^3
Molar absorptivity of photoinitiator	$\varepsilon = 20.0$ m^2/mol
Molar absorptivity of UV absorber	$\varepsilon = 2000.0$ m^2/mol
Reflective index of HDDA	1.40
Refractive index of silica	1.56
Refractive index of alumina	1.70
Refractive index of PZT	2.40
Total photon packet number	10^6
Laser wavelength	364 nm
Laser exposure time	500 ms

2. Physical modeling

In the ceramic μSL, the light scattering becomes significant when the light propagates through the highly concentrated ceramics suspension [15]. When a photon travels through the ceramic suspension, it is scattered by ceramic particles and its direction of propagation will be changed. Consequently, the photon is absorbed either by the UV-curable solution or the ceramic particles. The portion of the initial photons absorbed by the UV-curable solution will initiate the polymerization reactions. The multiple light scattering in highly concentrated ceramic suspensions is complicated and there is no available analytic solution to describe it. To ensure a better understanding of the multiple light scattering in concentrated ceramic suspensions, a numerical model based on the Monte Carlo ray tracing method is developed [15]. This model is coupled with the finite difference method to simulate the ceramic μSL process.

This numerical model consists of two parts: the light scattering by Monte Carlo simulation and the photo-polymerization by the finite difference method [15]. By repeatedly sampling values from the probability distributions for the uncertain variables, the Monte Carlo ray tracing techniques are applied to simulate the multiple light scattering on a ray-by-ray basis. The behavior of individual photons is simulated numerically. Photons are statistically generated according to the characteristics of the laser beam used in ceramic μSL. When a photon propagates in a concentrated ceramic suspension, there exists a certain probability of hitting a ceramic particle. This probability is determined by the mean free path of the photon in the ceramic suspensions. Once the photon hits the ceramics particle, it will be scattered and the scattering behavior is described by the Mie theory [16]. The calculations of propagation and scattering are repeated until the photon has been absorbed either by a ceramic particle or by the resin. Once the absorption profile attributed to the photoinitiator is obtained by the Monte Carlo simulation, the detailed micro-scale photo-polymerization is numerically calculated. A set of differential equations are used to describe the photo-polymerization processes [17]:

$$\frac{\mathrm{d}I}{\mathrm{d}z} = -\varepsilon[S]I \qquad \text{attenuation of light}$$

$$\frac{\mathrm{d}[S]}{\mathrm{d}t} = -\psi\varepsilon[S]I \qquad \text{photoinitiation}$$

$$\frac{\mathrm{d}[M]}{\mathrm{d}t} = -k_\mathrm{p}[R^\bullet][M] \qquad \text{propagation}$$

$$\frac{\mathrm{d}[R^\bullet]}{\mathrm{d}t} = \phi\varepsilon[S]I - k_\mathrm{t}[R^\bullet]^2 \qquad \text{termination}$$

Percentage of monomer conversion is used as a measure of the polymerization in this model. Using experimental data of reaction kinetics [18], the simulation reveals important characteristics in micro-scale photo-polymerization.

Using the developed numerical code [15], the influences of the following physical properties of ceramic particles and resin on the spatial resolution of the ceramic μSL are investigated: (1) particle size distribution; (2) refractive index of ceramic particle; (3) refractive index of UV-curable solution; (4) absorption coefficient of ceramic particles.

In general, the ceramic particles used in ceramic μSL always have a certain size distribution. According to the light scattering theory, both particle mean size and distribution affect the light scattering. In a typical ceramic μSL process, the mean size of the ceramic particles is varied from 0.3 to 1 μm. Strong light scattering will occur when the particle size is close to the wavelength of UV light (0.364 μm). Therefore, the influence of ceramic particle size on the light scattering and ultimately, resolution of μSL is carefully studied.

The particle size distribution is modeled by the Gaussian distribution (Fig. 3)

$$p(d) \propto p_0 \, \mathrm{e}^{-((d-d_0)/\Delta d)^2}$$

where p_0 is the total number of particles, Δd the Gaussian radius of particle size distribution, d_0 the mean size of the particles, and $p(d)$ is the number of particles with diameter d. In the numerical simulation, the diameter of an individual ceramic particle is randomly generated according to the distribution. The angular distribution patterns of scattered photons are calculated for each particle with various sizes in the numerical simulation.

According to the scattering theory, the scattered light is also determined by the refractive index difference at the interface of two different media. This phenomenon has been observed in the μSL fabrication of PZT ceramics, which has a high refractive index of 2.4 [10]. The strong scattering effect caused the poor lateral resolution and shallow curing depth, which reduced the bonding between layers. Therefore, refractive index contrast between ceramic particles and UV-curable solution is studied. The absorption coefficient of the ceramic particle, which is the imaginary component of the refractive index, remarkably changes the scattering light distribution [19]. The numerical code is modified to calculate the scattering pattern with a complex refractive index.

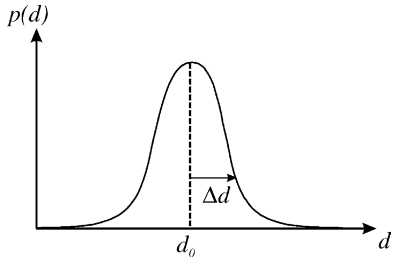

Fig. 3. The size variation of the ceramic particles can statistically be modeled by the Gaussian distribution. The $p(d)$ represents the number of particles with a given diameter d. The d_0 and Δd are the mean size of ceramic particles and the Gaussian radius of particle size distribution, respectively.

3. Results and discussion

3.1. The influences of the particle size and its distribution on ceramic μSL

Fig. 4 shows the curing depth and radius of a polymerized cone dot, which is formed from a single exposure of ceramic suspension, as a function of particle mean size from 0.3 to 1 μm. The curing depth increases with the particle mean size while the curing radius decreases. It indicates that the light scattering effect becomes significant when the particle size approaches the illuminated light wavelength. As the scattering effect becomes stronger, the incident photons will more likely be scattered into the surrounding area and consequently, fewer photons can penetrate deeper. Therefore, the polymerized cone dot has a larger radius and shallower depth. The result suggests that a particle size larger than 0.5 μm is preferred to eliminate the scattering effect in the ceramic μSL.

The particle size distribution dependence of the ceramics μSL resolution with the fixed mean size of 0.5 μm is shown in Fig. 5. When Δd increases from 0.05 to 0.30 μm, the curing depth decreases from 68 to 48 μm, whereas the curing radius increases from 4.7 to 7.8 μm. The simulation results suggest that strong light scattering occurs with larger particle size distribution. A larger particle size distribution means more particles with a size close to the laser wavelength are being used in ceramic μSL.

The stronger scattering effect resulting from broader particle size distribution results in poor spatial resolution. A narrow size distribution of ceramic particles is desired for fine ceramic μSL fabrication.

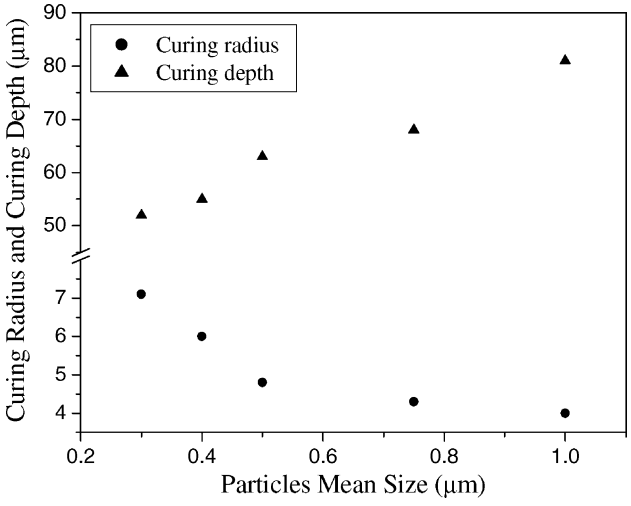

Fig. 4. Curing depth and curing radius as a function of particle mean size.

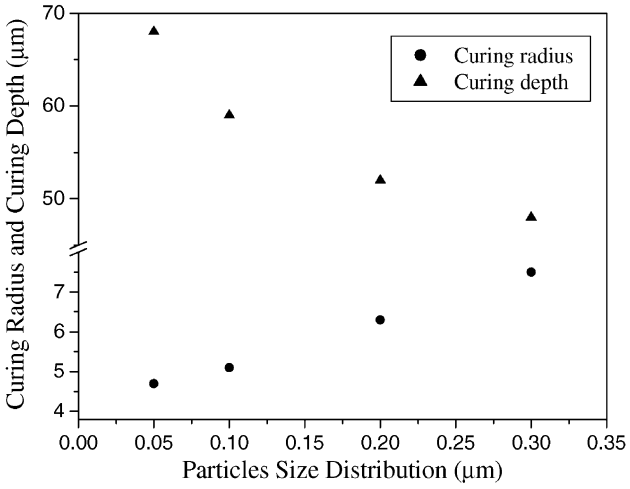

Fig. 5. Curing depth and curing radius as a function of particle size distribution Δd from 0.05 to 0.30 μm with fixed mean particle size of 0.5 μm.

3.2. The influences of the refractive indices of the ceramic particle and the resin on ceramic μSL

Fig. 6 shows the curing depth and radius dependence on the refractive index of ceramic particle suspended in the UV-curable resin, with the refractive index of 1.4. The curing radius increases from 4.3 to 8.2 μm, whereas curing depth decreases from 72 to 48 μm with an increase of refractive index of ceramic particle from 1.7 to 2.7. These results indicate that a larger difference in refractive index will produce a stronger scattering effect, which is agreed with the light scattering theory.

The scattering effect in ceramic μSL can be greatly minimized by choosing the ceramic particles that have the refractive index close to that of the solution. For certain applications, the ceramic material is often selected and cannot be replaced by other materials with smaller refractive indices. For example, in order to fabricate a Piezo actuator by ceramic μSL, PZT particles have to be used even its refractive index is as high as 2.4. According to the Mie theory, the light scattering in μSL is mainly determined by the refractive index contrast between ceramics particles and UV-curable solution. In order to reduce the scattering effect, an alternative method is to increase the refractive index of the UV-curable resin by additives of high refractive index [20]. By choosing the additive that does not change the chemical properties of the UV-curable solution, the μSL of high refractive index ceramics materials have been investigated with various refractive index of monomer resin [9].

Fig. 7 shows that the curing depth increases from 50 to 74 μm with an increase of the refractive index of UV-curable resin from 1.6 to 2.2, whereas curing radius decreases from 7.3 to 4.3 μm. This result confirms that the increase of the refractive index of UV-curable solution can effectively suppress the scattering effect.

3.3. The influences of the absorption coefficient of the ceramic particle on ceramic μSL

As shown in Fig. 8, both the curing depth and radius decrease with increases of the absorption coefficient of ceramic particles. The higher the absorption coefficient of the ceramic particle is, the more laser energy is absorbed. Therefore, less energy can be used for the photo induced polymerization. It suggests that higher laser intensity is required in the μSL of absorbing ceramic particles to maintain a certain curing depth.

3.4. Simulation on μSL of three common ceramics: silica, alumina, and PZT

Three representative ceramic materials used in μSL are chosen as case studies for numerical modeling: (1) silica as a low refractive index ceramic material; (2) alumina as a medium refractive index structural ceramic material; (3)

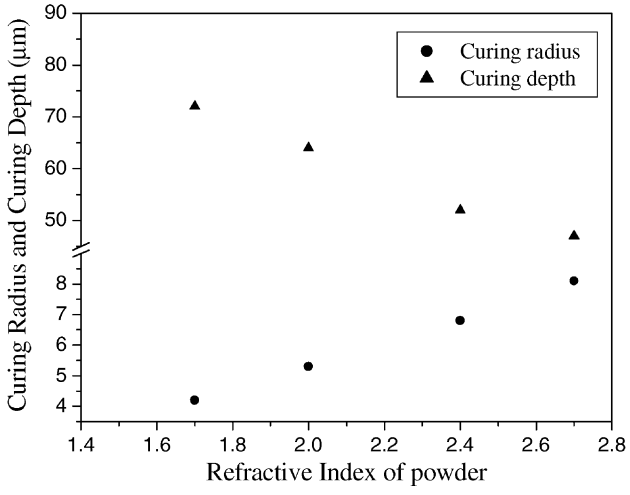

Fig. 6. Curing depth and curing radius as a function of refractive index of ceramic particle suspended at the UV-curable solution with $n = 1.4$.

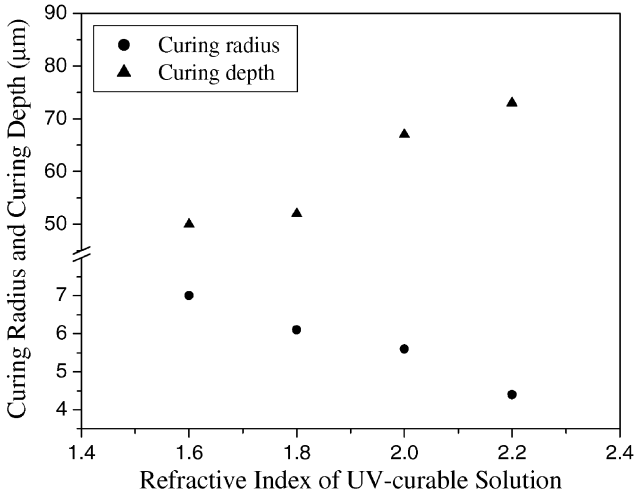

Fig. 7. Curing depth and curing radius as a function of refractive index of UV-curable solution. The refractive index of ceramics particle is 2.4.

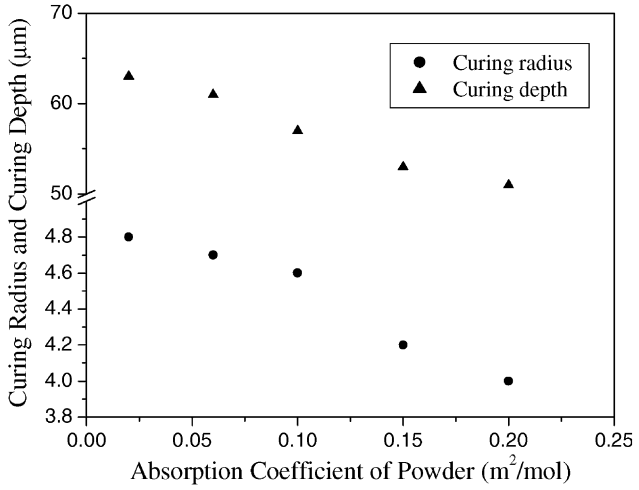

Fig. 8. Curing depth and curing radius dependence of absorption coefficient of ceramic particle.

Table 2
Refractive index and mean diameter of three ceramic powders

	Refractive index	Mean diameter (μm)
Silica[a]	1.56	2.28
Alumina[b]	1.70	0.38
PZT[c]	2.40	1.00
UV-curable resin	1.4	–

[a] α-Quartz, Atlantic equipment engineering.
[b] RC-HP, Reynolds.
[c] EDO 76.

PZT as a high refractive index ceramic material used as a functional material [20]. The refractive indices and mean diameters of three ceramic powders are listed in Table 2. UV-curable resins used to mix with three types of particles to form ceramic suspensions are the same with a refractive index of 1.4.

With an intensified laser beam, an increase of both curing depth and radius of μSL is observed for all three ceramic suspensions (Fig. 9). The alumina has the largest curing

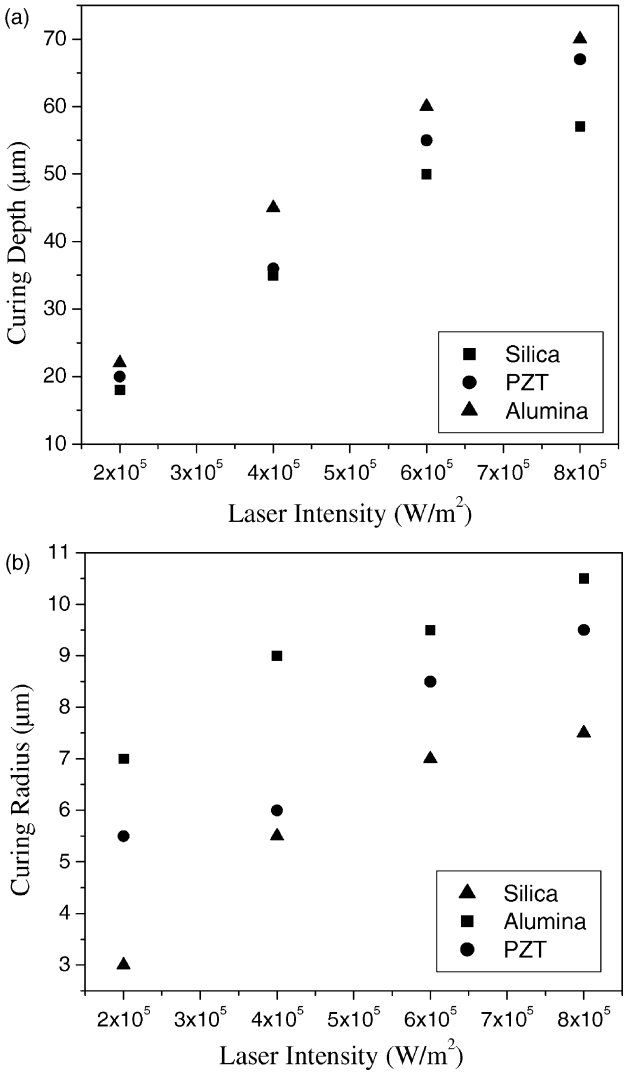

Fig. 9. (a) Curing depth and (b) curing radius as function of laser intensity of silica, alumina and PZT.

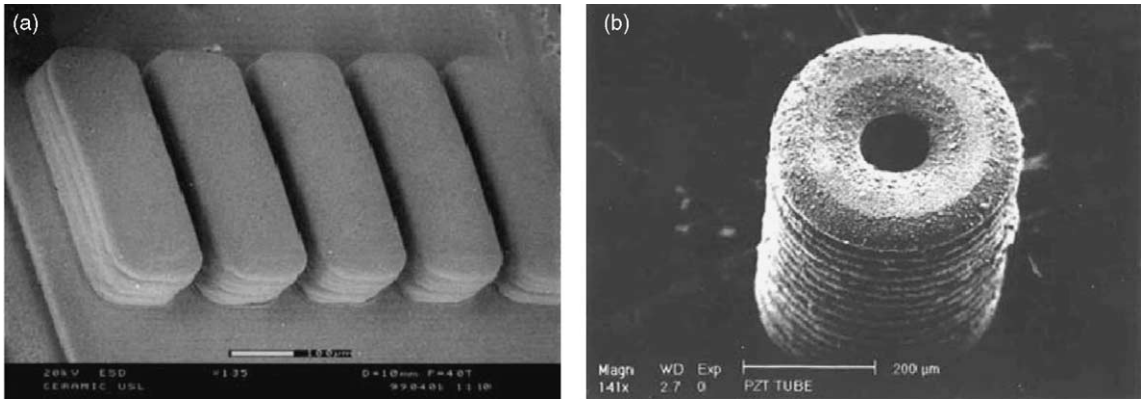

Fig. 10. Microfabrication of ceramic green structures: (a) 30 μm wide Al_2O_3 micro channels build by five layers with a layer thickness of 100 μm. The length of the channel is 400 μm; (b) the 400 μm high PZT micro tube is constructed by 20 layers with a layer thickness of 20 μm. The micro tube has the inner diameter of 100 μm and outer diameter of 350 μm.

radius and the smallest curing depth among all three ceramic materials. It is attributed to the stronger light scattering occurred for alumina suspension because the mean diameter of the particles (0.3 μm) is close to the UV laser wavelength (0.364 μm). On the other hand, a small refractive index and large diameter of silica particle leads to a weaker scattering during the fabrication, resulting in a larger curing depth and smaller curing radius.

The optical scattering during ceramic μSL is a rather complicated phenomenon and is collectively dependent on different physical parameters including particle size and optical properties of both particles and resin. The numerical modeling is demonstrated to be an effective method to simulate and optimize ceramic μSL process.

4. Microfabrication

By applying the numerical model to predict the critical process parameters, the micro green structures formed by various structural or functional ceramic materials have been successfully fabricated (Fig. 10). The 30 μm wide alumina micro channels are built by five layers with a layer thickness of 100 μm (Fig. 10(a)). The micro channels are 400 μm long and 100 μm high. The PZT micro tube shown in Fig. 10(b) has an inner diameter of 100 μm and outer diameter of 350 μm. The 400 μm high PZT micro tube is constructed by 20 layers, with a layer thickness of 20 μm.

5. Conclusion

The influences of critical physical properties of ceramic particles and UV-curable resins used in ceramic μSL are investigated through the developed numerical model. Light scattering is found to essentially influence the μSL of ceramics. It is found that the scattering is the strongest when the size of the ceramic powders approaches the laser wavelength (0.364 μm). It is also found that strong scattering occurs at a high refractive index contrast between the particle and the resin. High laser intensity is required to fabricate high UV absorption ceramic materials to compensate for the laser energy absorbed by the ceramic particles. μSL of three commercially available ceramics: silica, alumina and PZT, are examined by numerical model. The numerical modeling is demonstrated as an efficient method to predict the critical process parameters, and the high precision ceramic μSL has been achieved experimentally.

Acknowledgements

This work was supported by the Office of Naval Research under contracts #N00014-01-1-0803 and N00014-02-1-02240 and the National Scientific Foundation, award #DMI-0196395.

References

[1] J.M. English, M.G. Allen, Wireless micro-machined ceramic pressure sensors, in: Proceedings of the 12th IEEE International Conference on Micro Electro Mechanical Systems, Orlando, FL, January 17–21, 1999, pp. 511–516.
[2] H.H. Bau, S.G.K. Ananthasuresh, J.J. Santiago-Aviles, J. Zhong, M. Kim, M. Yi, P. Espinoza-Vallejos, L. Sola-Laguna, Ceramic tape-based meso systems technology, ASME MEMS'98, DSC V 66 (1998) 491–498.
[3] A.H. Epstein, S.D. Senturia, G. Anathasuresh, A. Ayon, K. Breuer, K.S. Chen, F.E. Ehrich, G. Gauba, R. Ghodssi, C. Groshenry, Power MEMS and microengines, in: Proceedings of the 1997 International Conference on Solid-State Sensors and Actuators, Part 2, vol. 2, Chicago, IL, June 16–19, 1997, pp. 753–756.
[4] D.L. Polla, L.F. Francis, Ferroelectric thin films in microelectro-mechanical systems applications, MRS Bull. 21 (1996) 59–65.
[5] C. Van Hoy, A. Barda, M. Griffith, J.W. Halloran, Microfabrication of ceramics by co-extrusion, J. Am. Ceram. Soc. 81 (10) (1998) 152–158.
[6] H.D. Chen, K.R. Udayakumar, L.E. Cross, J.J. Bernstein, L.C. Niles, Dielectric, ferroelectric, and piezoelectric properties of lead zirconate titanate thick films on silicon substrates, J. Appl. Phys. 77 (7) (1995) 3349–3353.
[7] J. Akedo, M. Ichiki, K. Kikuchi, R. Maeda, Jet molding system for realization of three-dimensional micro-structures, Sens. Actuators A 69 (1998) 106–112.
[8] Y. Hirata, H. Makaishi, T. Numazawa, H. Takada, Piezocomposite of fine PZT rods realized with synchrotron radiation lithography, IEEE Ultrason. Symp. 2 (1997) 877–881.
[9] X. Zhang, X.N. Jiang, C. Sun, Micro-stereolithography of polymeric and ceramic microstructures, Sens. Actuators A 77 (2) (1999) 149–156.
[10] X.N. Jiang, C. Sun, X. Zhang, Micro-stereolithography of 3D complex ceramic microstructures and PZT thick films on Si substrate, ASME MEMS 1 (1999) 67–73.
[11] P.F. Jacobs, Rapid Prototyping and Manufacturing: Fundamentals of Stereolithography, Society of Manufacturing Engineers Publishers, Dearborn, 1992.
[12] M.L. Griffith, J.W. Halloran, Ultraviolet curable ceramic suspensions for stereolithography of ceramics, Manuf. Sci. Eng. 2 (1994) 529–534.
[13] M.L. Griffith, J.W. Halloran, Free form fabrication of ceramics via stereolithography, J. Am. Ceram. Soc. 79 (1996) 2601–2608.
[14] C. Hinczewski, S. Corbel, T. Charier, Stereolithography for the fabrication of ceramic three-dimensional parts, Rapid Prototyping J. 4 (1998) 104–111.
[15] C. Sun, X. Zhang, Experimental and numerical investigations on micro-stereolithography of ceramics, J. Appl. Phys., in press.
[16] H.C. van de Hulst, Light Scattering by Small Particles, Wiley, New York, 1957.
[17] G. Odian, Principles of Polymerization, McGraw-Hill, New York, 1970.
[18] L. Flach, R. Chartoff, A process model for nonisothermal photopolymerization with a laser light source. I. Basic model development. II. Behavior in the vicinity of a moving exposed region, Polym. Eng. Sci. 35 (6) (1995) 483–498.
[19] P.W. Barber, S.C. Hill, Light Scattering by Particles: Computational Methods, World Scientific, Singapore, 1990.
[20] M.L. Griffith, J.W. Halloran, Scattering of ultraviolet radiation in turbid suspensions, J. Appl. Phys. 81 (1997) 2538–2546.

Biographies

Cheng Sun graduated with PhD in Industrial Engineering from Pennsylvania State University in 2002 and MS/BS in Physics from

Nanjing University. He is currently working as the research assistant in the Micro-manufacturing Laboratory (μML) at University of California at Los Angeles. His past research experiences include: kinetics of low dimensional crystal growth, high-T_c superconductivity. His current research interests are: micro-nano scale engineering, novel 3D fabrication technologies, laser processing.

Xiang Zhang graduated with PhD in Mechanical Engineering from University of California, Berkeley in 1996 and MS/BS in Physics from Nanjing University. He joined University of California at Los Angeles in 2000 as an associate professor and directs UCLA's Micro-manufacturing Laboratory (μML). His past research experiences include: micro thermal wave sensor design and fabrication, ferroelectric liquid crystal phase transition, high-T_c superconductivity, laser processing of semiconductor materials. His current research interests are: micro-nano scale engineering, novel 3D fabrication technologies in microelectronics and photonics, micro and nano-devices, nano-lithography and nano-instrumentation, rapid prototyping, bio-MEMS, and semiconductor manufacturing.